# A New Method for Label-Free Imaging of Biomolecular Interactions

**Peter Y. Li, Bo Lin, John Gerstenmaier, and Brian T. Cunningham**

SRU Biosystems
14A Gill Street, Woburn, MA 01801, USA
pli@srubiosystems.com

## Abstract

*A new method for producing label-free high-resolution images of biomolecular binding to the surface of a biosensor is demonstrated. The biosensor incorporates a guided mode resonance filter that, when illuminated with white light, is designed to reflect only a narrow band of wavelengths where the reflected wavelength is tuned by the adsorption of biological material onto the sensor surface. In this work, an instrument is used to acquire spatial maps of the resonant reflected wavelength in order to produce images of bound biomolecule patterns as applied by a microarray spotter. The biosensor imaging capability is expected to yield applications in pharmaceutical compound screening, genomics, proteomics, and molecular diagnostics, where there is a need to screen large numbers of biochemical interactions against samples using low volumes of reagents.*

## Keywords

Optical biosensor, label-free, imaging, SPR

## INTRODUCTION

The need to measure increasingly large numbers of biochemical interactions is currently being driven by several industries. The ability to detect the interactions between sets of DNA probes arrayed on to glass surfaces and test samples are used for genotyping, gene expression analysis, and gene sequencing[1][2]. Likewise, arrays of hybridized protein probes are finding applications in protein pathway analysis[3], and protein expression diagnostic tests[4]. The concept of parallel detection of sample interaction with an array of hybridized probes is further expanding into small molecule screening for pharmaceutical discovery, environmental testing, and others.

While these array-based techniques are able to provide a high density of probes, detection of molecular hybridization to the probes from the test sample is typically accomplished through the attachment of a label. Common labels are radioisotopes, fluorophores, enzyme substrates, or haptens.

In contrast with the large variety of labeled methods, there are relatively few methods that allow detection of molecular and cellular hybridization without labels. Label-free detection removes experimental uncertainty induced by the effect of the label on molecular conformation, blocking of active binding epitopes, steric hindrance, inaccessibility of the labeling site, or the inability to find an appropriate label that functions equivalently for all molecules in an experiment. Label-free detection methods greatly simplify the time and effort required for assay development, while removing experimental artifacts from quenching, shelf life, and background fluorescence.

Label-free detection methods include surface plasmon resonance (SPR), grating couplers, ellipsometry, evanescent wave devices, reflectometry, interferometry, and gravimetry[5]. Of these methods, only SPR-based and ellipsometry-based techniques have demonstrated the capability for producing high resolution images of molecular binding in a hybridization array format[6][7]. SPR-imaging methods rely upon hybridization of probes to a gold surface, and are capable of gathering information from a ~1x2 $cm^2$ area due to limitations of the laser illumination source, light coupling optics, and uniformity of the sensor[8][9]. SPR-imaging instruments using the Kretschmann configuration require rotation of the sample stage to find an optimal observation angle for a given sample, so that all the hybridization locations can be tuned to the resonance condition, thus requiring all receptor probes to be applied with identical density. While the effectiveness of SPR-imaging has been demonstrated for small arrays of oligonucleotides[10][11], and large-molecule proteins, broad commercial acceptance of SPR-imaging systems has been hindered by their limitations[12].

In previous work, we have developed a novel technology based upon a narrow bandwidth guided mode resonant filter structure that has been optimized to perform as a biosensor[13][14][15]. The sensor utilizes a sub-wavelength grating structure that produces a particular diffraction anomaly providing a surface that, when illuminated with white light at normal incidence, reflects only a very narrow (resonant) band of wavelengths. The resonantly reflected wavelength is shifted by the attachment of biomolecules to the guided mode filter, so that small changes in surface optical density can be quantified without attachment of a label to the detected biomolecule. Equivalent sensor structures have been fabricated onto glass substrates and incorporated into sheets of plastic film. Previous results demonstrate the ability to produce the biosensor in plastic over large surface areas and the incorporation of the sensor into large area disposable assay formats such as microtiter plates and microarray slides[14].

Previously described biosensor readout instrumentation utilized a white light source illuminating a ~1 mm diameter region of the sensor surface through a 100 to 400 micron

0-7803-8133-5/03/$17.00 ©2003 IEEE

diameter optical fiber and a collimating lens at nominally normal incidence. A detection fiber is bundled with the illumination fiber for gathering reflected light for analysis with a single-point spectrometer. Detection multiplexing was performed through simultaneous readout from multiple illumination/detection heads. For each measurement, a peak wavelength value (PWV) is determined, and the PWV shift between two measurements is determined by subtracting the PWV of the sensor in a reference state (such as before an experiment begins) from the PWV of the sensor in its current state.

In this work, we demonstrate an imaging system that is capable of generating high-resolution spatial maps of the PWV on our biosensor surface. Using this instrument, it is possible to observe patterns of biomolecule receptor attachment and hybridization interactions with high density. As the same biosensor structure and peak-detecting method are used for single-point-based and imaging-based detection, the sensitivity (in terms of amount of PWV shift observed and resolution of PWV shift detection) of the approach is not compromised.

## MATERIALS AND METHODS

### Imaging Instrument

A schematic diagram of the biosensor PWV imaging instrument is shown in Figure 1. White light (Oriel quartz tungsten halogen lamp, 20 W) illuminates the sensor at normal incidence, with a polarization filter to apply only light with polarization direction perpendicular to the sensor grating lines. The reflected light is directed through a beam splitter and an imaging lens of unity magnification to a narrow slit aperture at the input of an imaging spectrometer (Jobin Yvon Triax550). The width of the slit may be set at a desired value, e.g., within a range from 6 microns to 200 microns. Using this method, reflected light is collected from a line on the sensor surface, where the width of the imaged line is determined by the width of the entrance slit of the imaging spectrometer. The imaging spectrometer contains a 2-dimensional CCD camera with 2048 x 512 pixels. The line of reflected light, containing the biosensor resonance signal, is diffracted by a diffraction grating to produce a spatially-resolved spectrum from each point within the line. When the CCD camera is operated in 2048 x 512 pixel mode, the line-image through the slit is imaged onto 512 pixels. A spectrum, with a resolution of 2048 wavelength data points, is acquired for each of the 512 pixels. Upon peak-finding analysis of all 512 spectra, the PWVs of 512 pixels are determined. Thus a line of 512 pixels is generated for the PWV image of the sensor.

To generate a two-dimensional image of the sensor, a motorized stage translates the sensor in the direction that is perpendicular to the image line. The spatial separation of the image lines is determined by the step-size of the stage between each image-line acquisition. (In addition, the CCD can be read out with various resolutions by binning pixels.) By this technique, a series of lines are assembled

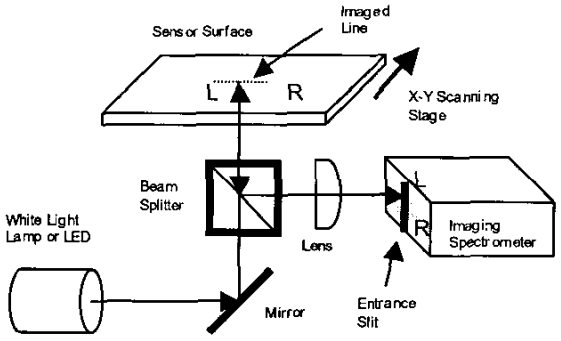


**Figure 1 Schematic diagram of the BIND imaging system used for this study**

into an image through software. In the current system, the length of the image-line is 6.9 mm, as determined by the size of the CCD chip, across the biosensor surface. A large area can be scanned in a tiled fashion, where the width of a tile is 6.9 mm, by translating the sensor in steps of 6.9 mm along the image-line direction.

Typically, a biosensor experiment involves measuring shifts in PWV, so the sensor surface is scanned twice, once before and once after biomolecular binding, and the images are aligned and subtracted to determine the difference in PWV as detected by the sensor. This scanning method does not require the PWV of the imaged surface to be completely uniform, either across the surface or within a set of probe locations, or tuning of the sensor angle to a resonance condition as with SPR-imaging.

### Sensor Fabrication

The sensor structure utilizes a grating with a period lower than the wavelength of the resonantly reflected light[16][17]. Structures reported in this work utilized a linear grating with a period of 500 nm and a depth of ~170 nm. The grating was micro-replicated from an etched silicon wafer with a negative of the sensor surface structure acting as a mold for a layer of ultraviolet-light-cured resin that is squeezed between the silicon and a polyester sheet, as described in a previous publication[14]. After the resin is cured, the solid surface structure is peeled away from the silicon wafer, and stays adhered to the polyester sheet. Sensor fabrication is completed by sputter deposition of a high refractive index dielectric coating of tantalum oxide.

### $NH_2$ Surface Activation Protocol

Where indicated, some of the sensors were activated with amine functional groups to enable various bifunctional linker molecules to be attached to the surface in a known orientation. Amine activation was performed by immersion of the sensor in 10% 3-aminopropyltriethoxysilane (Pierce) solution in ethanol (Aldrich) for 1 min, followed by a brief ethanol rinse. Activated sensors were then dried at 70°C for 10 min.

### Assay Protocol

N-hydroxysuccinimide linkers NHS-PEG and NHS-PEG-biotin were purchased from Shearwater and used according to manufacturer's instruction. Cy5-labeled streptavidin was ordered from Molecular Probe. All other proteins were ordered from Sigma and diluted with water or PBS to desired concentration for coating the sensor surface or for detecting protein-protein interaction. Protein coating and protein binding reaction were carried out at room temperature.

The collagenase activity assay was done by first immobilizing gelatin on the sensor surface, and then collagenase was added to the final concentration of 3 μg/ml in reaction buffer that contains 100 mM Tris-HCl, 200 mM NaCl, and 5 mM $CaCl_2$ pH 7.6. After incubating for 60 min at room temperature, collagenase solution was replaced with reaction buffer and washed thoroughly with PBS buffer. The enzyme activity was continually monitored by the detection system during the incubation time and the endpoint was analyzed after PBS wash. Collagenase substrate specificity study was also performed, in which the enzymatic activity was carried out on the sensor surface coated with rabbit IgG.

## RESULTS

### Surface Patterning with Proteins

The following experiment was performed to demonstrate image-based detection of PWV in an assay that could be performed in parallel by fluorescence imaging, and to demonstrate the equivalence of PWV shift for the image-based readout instrument compared to the single-point readout instrument.

A guided mode filter biosensor was prepared with a silicon oxide dielectric top surface, as described above, and surface activated with $NH_2$ binding groups. The sensor was bonded with adhesive to the bottom of a conventional bottomless 96-well microtiter plate.

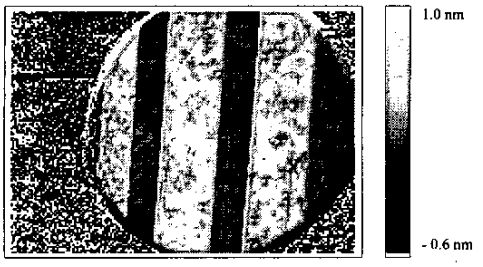


**Figure 2 Biotin-patterned surface within a 9mm diameter microtiter plate well used to detect Cy-5 labeled streptavidin measured using the biosensor imaging instrument. Light regions indicate where biotin was applied, resulting in areas of highest binding of Cy5-streptavidin.**

Three vertical stripes of NHS-PEG-Biotin (Shearwater) were applied by dispensing three separate 1 μl volume of 1 mg/ml NHS-PEG-Biotin droplets with a micropipette tip, and manual spreading of the droplets. The NHS-PEG-Biotin solution was allowed to incubate on the sensor surface for 20 minutes before thorough rinsing with deionized water. Next, the sensor surface was immersed in 50 μl of 1 mg/ml NHS-PEG solution (Shearwater) and allowed to incubate for an additional 20 minutes. The NHS-PEG molecule preferentially attaches to regions of the sensor with unreacted surface $NH_2$ groups, and blocks nonspecific interaction of proteins with the regions of the sensor that were not exposed to the NHS-PEG-Biotin. After an additional thorough rinse with deionized water, a baseline PWV image was scanned at 50 μm resolution. Next, the sensor surface was immersed in 50 μl of Cy5-labeled streptavidin (Molecular Probe) at a concentration of 1 μg/ml, and allowed to incubate for 30 minutes before a final rinse with water. A second PWV image was also scanned at 50 μm resolution. Figure 2 shows the PWV shift image obtained by subtracting the initial PWV image from the PWV image obtained after streptavidin-Cy5 binding. (Only the area within the circle is the sensor area.) Light regions represent areas of greater PWV shift, where the streptavidin-Cy5 selectively attached to the immobilized NHS-PEG-Biotin molecules, while dark regions represent areas of low PWV shift, where the immobilized NHS-PEG block attachment of streptavidin-Cy5. The average PWV shift in the light areas was 0.48 nm, while the average PWV shift in the dark areas was 0.03 nm. The ~0.5 nm shift in PWV due to streptavidin binding is consistent with that measured using the single point spectrometer[13].

### Protein Array: Antibody-Antigen Interaction

A second experiment was performed to demonstrate application of a small array of IgG molecules using a conventional pin-based microarray spotter, and differential affinities of the spotted proteins to a test protein. The sensor had a tantalum oxide dielectric surface, and was bonded with optical adhesive to the top surface of a conventional 1x3-inch glass slide. Before application of spots, a baseline PWV image was taken at 50 μm resolution with the sensor surface covered with deionized water.

Using 4 different types of IgG (rabbit, chicken, goat, and human) at 1mg/ml concentration, 4 rows with 7 replicate columns were applied as shown in Figure 3a. Using a commercially available pin-and-ring based microarray spotter (Genetic MicroSystems, GMS 417 Arrayer), the proteins produce spots of ~400 μm diameter with a center-to-center spacing of 800 μm. The spots were allowed to incubate on the sensor surface at room temperature for 20 minutes, before the sensor was rinsed with deionized water. A second PWV image was taken over the region where the spots were applied, and a PWV-shift map, shown in Figure 3a, was obtained by subtracting the first PWV image from the second PWV image. Lighter regions indicate areas with greater PWV shift. The deposited IgGs result in an average positive PWV shift of 1.0 nm.

Next, the sensor surface was immersed in a 1 mg/ml solution of gelatin in PBS for 30 minutes to block nonspecific binding of the test solution with the regions not containing spots. After rinsing in PBS, a second baseline PWV image was measured, before exposure of a 100 μg/ml solution of anti-human IgG (Sigma) to the entire surface for 30 minutes. After a final PBS rinse, a fourth PWV image was scanned, and subtracted from the second baseline image to produce the PWV-shift map shown in Figure 3b. In Figure 3b, the anti-human IgG interacts only with the human-IgG spots, with an average PWV shift of 0.5 nm. The spot locations containing other IgG molecules measured no discernable shift in PWV.

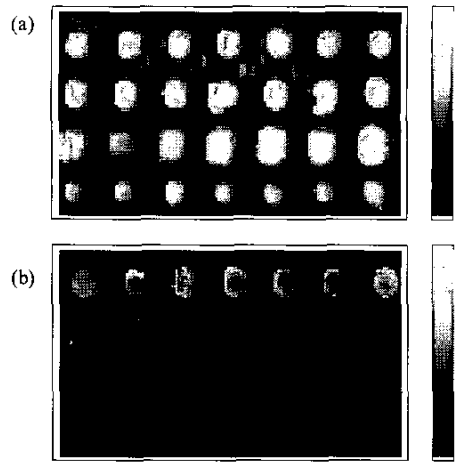


**Figure 3 PWV shift measured by the application of IgGs with ~400 μm diameter spots (a), and by subsequent exposure of the array to a solution containing anti-human IgG (b). The PWV shift represented by the gray scale bar is –0.2 nm to 1.5 nm, where light regions represent areas of greatest positive shift.**

### Protein Microarray: Specific Protein Binding and Cleavage

An experiment was performed to demonstrate that a high density array of receptors can be patterned on the surface of a biosensor within a microtiter plate well format to further increase the number of assays that can be performed in parallel. As shown in Figure 4a, alternating rows of ~400 μm diameter gelatin and rabbit IgG spots were applied to the surface of a tantalum oxide coated biosensor using a conventional microarray spotter (Genetic MicroSystems, GMS 417 Arrayer). (Gelatin spots are brighter than IgG spots in this figure.) Circles indicate areas corresponding to wells in a 96-well microtiter plate. (Spotting in this experiment was done on an unbonded sensor sheet.) Figure 4a shows an image of the PWV shift measured by subtracting a baseline PWV image scanned at 50 μm resolution before application of the spots from a PWV image scanned at the same resolution after application of the spots and thorough rinsing in PBS. The gelatin spots were applied from a 1 mg/ml concentration solution in PBS, while the rabbit IgG spots were applied from a 1 mg/ml solution in PBS. After washing, the gelatin spots retain more material than the IgG spots, as shown by their greater brightness in the PWV shift image. The gelatin spots had an average PWV shift of 0.89 nm, while the IgG spots registered an average PWV shift of 0.26 nm.

Following application of the spots, the sensor surface was immersed in 100 μl of a 1 mg/ml solution of cytochrome-C (Sigma) to apply a layer of protein on the non-spotted sensor regions to block subsequent nonspecific binding. The cytochrome-C solution was incubated on the sensor at room temperature for 30 min, followed by thorough rinsing with PBS. After rinsing, a PWV image was obtained, and the PWV values of the first baseline image were subtracted to produce the PWV-shift image shown in Figure 4b. While the PWV values in the spotted regions containing gelatin and IgG increased by 0.61 nm and 0.83 nm, respectively, the PWV in the unspotted regions increased by 1.05 nm due to the cytochrome-C binding.

Next, the sensor surface was immersed in 100 μl of 3 μg/ml of the enzyme collagenase for 60 min, and then rinsed again with PBS. Another PWV image was obtained, from which the original baseline PWV image was subtracted to produce the PWV shift image shown in Figure 4c. The collagenase specifically cleaves the gelatin from the gelatin spots, rendering the previously bright spots to an intensity that is close to the background (with PWV shift of –0.94 nm), while the PWVs within the IgG spots are less affected (with PWV shift of –0.31 nm). The total negative PWV shift on gelatin spots due to cleavage roughly corresponds to the increased amount of PWV due to gelatin binding on the surface.

Finally, the sensor surface was immersed in 100 μl of 100 μg/ml anti-rabbit IgG in PBS for 30 min, and rinsed in PBS. As before, a PWV image was obtained, from which the original baseline PWV image was subtracted to produce the PWV shift image shown in Figure 4d. The previously dark spots where rabbit-IgG is present have registered a positive PWV shift, thus becoming brighter, while the PWV within the cytochrome-C regions and the gelatin regions (where the gelatin has been removed by collagenase) are unaffected. The average PWV shift measured for anti-rabbit IgG binding was 0.32 nm.

## DISCUSSION

The experimental results described in this work represent the first demonstration that biosensors based on the guided-mode resonant filter technology, like surface plasmon resonance, can be utilized for producing high resolution images of biomolecular binding patterns on a sensor surface.

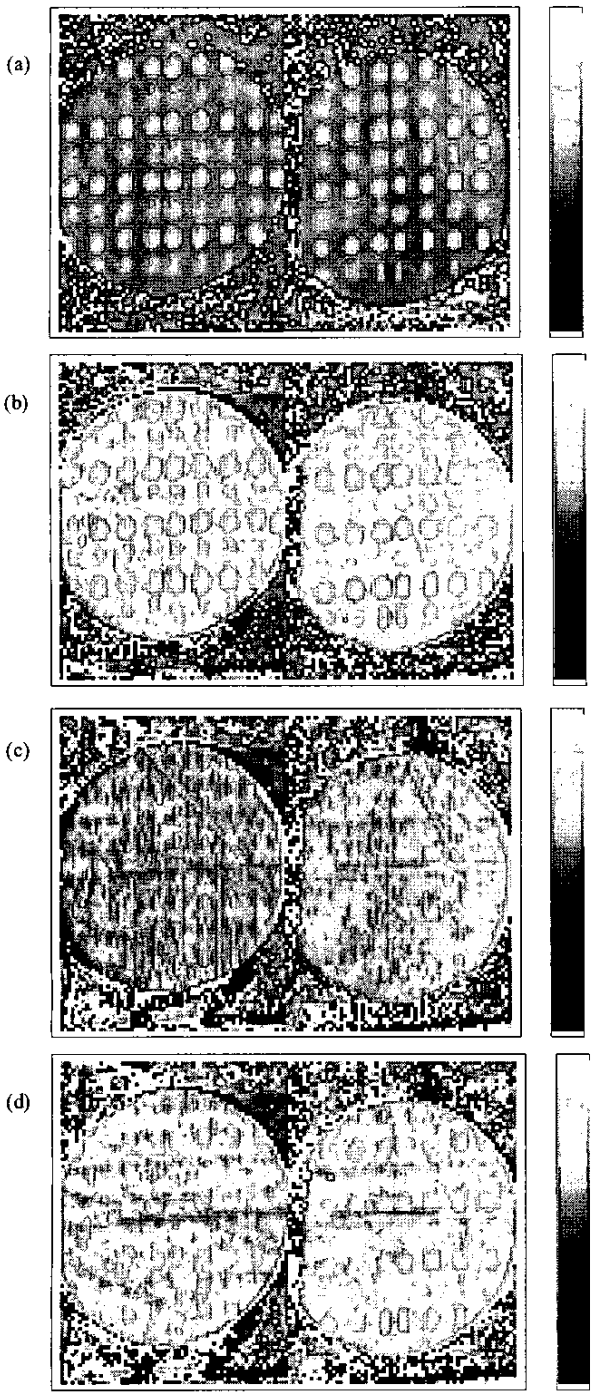


**Figure 4 Images of PWV shift due to (a) application of alternating rows of gelatin and rabbit IgG spots, (b) blocking of the surface with cytochrome-C, (c) selective cleavage of the gelatin by exposure to collagenase, and (d) selective binding of anti-rabbit IgG. The range of PWV shift shown on the gray scale bar is –2 nm to 2 nm.**

While future work will focus on determining detection sensitivity limits, results from these experiments show that the PWV shift measured from the imaging instrument for binding of a protein monolayer is consistent with that measured using the single-point spectrometer detection method used in previous research. Further, because the imaging spectrometer measures equivalent resonance spectral width and spectral resolution as the single-point detection method, the resolution for detecting small shifts in PWV has been unaffected by performing image-based detection.

Future publications will also describe in more detail the fundamental limits of spatial resolution afforded by this approach. The imaging system described here has a spatial resolution of 13.5 μm. This level of resolution is adequate for many applications. A more fundamental limit of resolution will be imposed by the extent of lateral propagation of guided modes within the optical structure. The waveguiding properties of the structure are designed such that laterally coupled light cannot propagate freely for long distances, but rather to leak energy away through scattering against the grating and coupling with forward and reverse diffracted light. Guided mode resonant structures similar to the ones reported here claim theoretical light propagation distances of only 3-5 μm[18], which would pose a limit to differentiating binding at a smaller size scale. The extent to which the optical structure may be engineered to control the characteristic propagation distance is a subject under investigation.

## CONCLUSION

To conclude, we have demonstrated for the first time that a biosensor based on a guided mode resonant filter phenomenon can be used for generating high spatial resolution images of biomolecular binding, using an instrument with an imaging spectrometer. Because the same biosensor used for imaging studies is identical to the one used for single-point assays within microtiter plates, there is no difference in the detection signal or the detection resolution. We expect this capability to greatly simplify high density, high throughput screening assays that currently require colorimetric or fluorescent labels to spatially discriminate locations of highest/lowest biochemical binding on a patterned surface. While DNA microarrays and protein microarrays are products that will most readily utilize this capability, we envision extension of label-free high resolution pattern-based screening to drug compound screening, cell toxicity studies, protein biomarker diagnostic tests, and environmental detection.

## ACKNOWLEDGMENTS

The authors gratefully acknowledge the dedicated efforts of Brenda Hugh, Derek Puff, Frank Wang, Alex Borsody, and Frank DeFilippi at SRU Biosystems.

## REFERENCES


[1] S.P.A. Fodor, et. al. "Light-directed spatially addressable parallel chemical synthesis," *Science,* **251**, p. 767-773, 1991.

[2] S. Gingh-Gasson, R.D. Green, Y. Uye, C. Nelson, F. Blattner, M.R. Sussman, and F. Cerrina, "Maskless fabrication of light-directed oligonucleotide microarrays using a digital micromirror array," *Nature Biotechnology*, **17**, p. 974-978, 1999.

[3] B.B. Haab, M.J. Dunham, and P.O. Brown, "Protein microarrays for highly parallel detection and quantitation of specific proteins and antibodies in complex solutions," *Genome Biology*, **2**, no. 2, 2001.

[4] H. Zhu, et. al., "Global analysis of protein activities using proteome chips," *Science,* **293**, p. 2101-2105, 2001.

[5] A. Cunningham, "*Analytical Biosensors*," John Wiley & Sons, 1998.

[6] A.N. Grigorenko, A.A. Beloglazov, P.I. Nikitin, C. Kuhne, G. Steiner, and R. Salzer, "Dark-field surface plasmon resonance microscopy," *Optics Communications,* **174**, p. 151-155, 2000.

[7] G. Jin, P. Tengvall, I. Lundstrom, and H. Arwin, "A biosensor concept based on imaging ellipsometry for visualization of biomolecular interactions," *Anal. Biochem.*, **232**, p. 69-72, 1995.

[8] C.E. Jordan and R.M. Corn, "Surface plasmon resonance imaging measurements of electrostatic biopolymer adsorption onto chemically modified gold surfaces," *Anal. Chem.*, **69**, p. 1449-1456, 1997.

[9] P.I. Nikitin, A.N. Grigorenko, A.A. Beloglazov, M.V. Valeiko, A.I. Savchuk, O.A. Savchuk. G. Steiner, C. Kuhne, A. Huebner, and R. Salzer, "Surface plasmon resonance interferometry for microarray biosensing," *Sensors and Actuators A,* **85**, p. 189-193, 2000.

[10] C.E. Jordan, A.G. Frutos, A.J. Thiel, and R.M. Corn, "Surface plasmon resonance imaging measurements of DNA hybridization adsorption and streptavidin/DNA multilayer formation at chemically modified gold surfaces," *Anal. Chem.*, **69**, p. 4939-4947, 1997.

[11] A.J. Thiel, A.G. Frutos, C.E. Jordan, R.M. Corn, and L.M. Smith, "In situ surface plasmon resonance imaging detection of DNA hybridization to oligonucleotide arrays on gold surfaces," *Anal. Chem.*, **69**, p. 4948-4956, 1997.

[12] E. Zubritsky, "New Choices for SPR," *Anal. Chem.*, April 1, 2000, p. 289A.

[13] B.T. Cunningham, P. Li, B. Lin, J. Pepper, "Colorimetric Resonant Reflection as a Direct Biochemical Assay Technique," *Sensors and Actuators B,* **81**, p. 316-328, (2002).

[14] B. Cunningham, B. Lin, J. Qiu, P. Li, J. Pepper, and B. Hugh, "A plastic colorimetric resonant optical biosensor for multiparallel detection of label-free biochemical interactions," *Sensors and Actuators B,* **85**, p. 219-226, (2002).

[15] B.T. Cunningham, J. Qiu, P. Li, and C. Baird, "Enhancing the Surface Sensitivity of Colorimetric Resonant Optical Biosensors," *Sensors and Actuators B,* **87**, p. 365-370, (2002).

[16] R. Magnusson, and S.S. Wang, "New principle for optical filters," *Appl. Phys. Lett.*, **61**, No. 9, p. 1022, August, 1992.

[17] S. Peng and G.M. Morris, "Resonant scattering from two-dimensional gratings," *J. Opt. Soc. Am. A*, Vol. 13, No. 5, p. 993, May 1996.

[18] A. Hessel and A.A. Oliner, "A new theory of Wood's Anolmalies on Optical Gratings," *Applied Optics*, Vol. 4, No. 10, October 1965.